

# SPECTROSCOPY WITH ELECTRONIC TERAHERTZ TECHNIQUES FOR CHEMICAL AND BIOLOGICAL SENSING

MIN K. CHOI

*Department of Electrical & Computer Engineering  
University of Wisconsin -Madison  
1415 Engineering Drive  
Madison WI 53706-1691 USA  
mchoi@cae.wisc.edu*

KIMBERLY TAYLOR

*Biophysics Degree Program  
University of Wisconsin -Madison  
1415 Engineering Drive  
Madison WI 53706-1691 USA  
kmtaylor@students.wisc.edu*

ALAN BETTERMANN

*Department of Electrical & Computer Engineering  
University of Wisconsin -Madison  
1415 Engineering Drive  
Madison WI 53706-1691 USA  
adb@engr.wisc.edu*

DANIEL W. VAN DER WEIDE

*Department of Electrical & Computer Engineering  
University of Wisconsin -Madison  
1415 Engineering Drive  
Madison WI 53706-1691 USA  
danvdw@engr.wisc.edu*

By illuminating the sample with a broadband 10-500 GHz stimulus and coherently detecting the response, we obtain reflection and transmission spectra of common powdered substances, and compare them as a starting point for distinguishing concealed threats in envelopes and on personnel. Because these samples are irregular and their dielectric properties cannot be modulated, the spectral information we obtain is largely qualitative. To show how to gain quantitative information on biological species at micro- and millimeter-wave frequencies, we introduce thermal modulation of a globular protein in solution, and show that changes in microwave reflections coincide with accepted visible absorption spectra, pointing the way toward gaining quantitative chemical and biological spectra from broadband terahertz systems.

Keywords: electronic terahertz techniques, gas spectroscopy, reflection spectroscopy, nonlinear transmission lines, samplers, coherent measurements

## 1. Introduction

With the advent of short-pulse coherent measurement techniques, based either on optoelectronic or on purely electronic means of generating and detecting broadband radiation, researchers are now equipped with new tools for qualitative sensing and even quantitative measurement of chemical and biological entities. The possibility of using stand-off (i.e. non-contact stimulus/response measurements at a distance) techniques to assess the presence of chemical and biological weapons is of particular interest, and is an

application that is well-suited to wavelengths at the millimeter length scale, since these can penetrate clothing and envelopes while still forming images with useful spatial resolution.

Hence, this recent interest in sensing chemical and biological entities with frequencies in the megahertz through terahertz regime has brought about a growing body of experimental results, as well as raising curiosity about the fundamental interactions with, and effects of this broadband radiation on, biological samples.

Such samples can be classified by their phase—vapor, liquid or solid—as well as by their degrees of homogeneity and complexity—purified, admixture, or tissue. Furthermore, the interaction of sample volume and wavelength will set limits on and complicate the interpretation of broadband measurements. Many broadband pulsed systems have < 40 dB dynamic range, which limits the thickness of a highly-absorbing sample, while thin or more transparent samples will require a minimum interaction length with the radiation to produce meaningful contrast above the noise and non-repeatability of broadband systems. Because sample thickness is often commensurate with measurement wavelength, etalon effects of the sample, in which multiple quarter- or half-wave resonances modulate the detected signal, are often compounded with auxiliary standing-wave effects of the measurement apparatus and environment. While radiometric millimeter-wave techniques that rely on the sample's black-body radiation would minimize these standing wave effects, these are not broadband systems, nor do they illuminate the sample.

Thus, in contrast with traditional spectroscopy techniques in the infrared and visible, where sample size is typically much larger than the wavelength, probing chemical and biological samples with broadband terahertz radiation requires reconsideration and careful specification of the sample's physical characteristics. The confounding effects of these characteristics on the raw result usually require a differential (normalized) measurement technique to measure the actual sample behavior, and this can result in magnification of standing wave effects.

While we briefly survey the background of broadband sensing for chemical and biological samples, our principal focus here is on sensing solid-phase, condensed samples that are either pure or admixtures of known substances, typical of what might be expected in a concealed bulk (as distinct from trace) threat.

In addition, to advance an argument for better understanding of sample/radiation interactions, we discuss microwave spectroscopy of purified biomolecules in solution, in this case a globular protein, bovine pancreatic ribonuclease (RNase A), which we thermally denature (unfold) while simultaneously probing the sample with microwave and visible light. In this experiment, we gain two important advantages:

- We can externally modulate the sample (in this case the protein's conformation), and
- We can independently confirm our microwave measurement with an accepted optical technique.

Such modulation and independent, simultaneous confirmation is usually lacking in broadband measurements, making interpretation of the data more challenging.

Since, on the other hand, concealed threats are (almost by definition) not amenable to modulation, single-line or narrowband radiation is probably less useful for qualifying the

nature of the threat than is broadband radiation. Although it has more power, and microwave holography has been reported for imaging of concealed weapons,<sup>1</sup> narrowband illumination fundamentally restricts the availability of spectral information in a complex environment. Even with the richer spectrum of broadband radiation, the lack of independent confirmation of contrast mechanisms (such as an optical spectroscopic probe) leaves us with few choices other than to look for characteristic patterns in the broadband reflection or transmission spectra that we measure. The coherence of these synchronous generation/detection spectrometers enables us to measure both magnitude and phase of transmission and reflection. While a characteristic spectral pattern can emerge in the phase spectrum, there is still more progress to be made in quantifying these spectra.

Nonetheless, having millimeter-scale spatial resolution and GHz-level spectral resolution enables qualitative identification of features that, in a pattern-matching algorithm, can be applied to a form of spectroscopic imaging for security screening. Thus the main results presented here are spectra that might be further processed by such an algorithm to result in a false-color image that would indicate the presence of unusual (chemical or biological) substances concealed within envelopes or under clothing.

## 2. Background

Broadband microwave spectrometers or network analyzers, whether time-<sup>2</sup> or frequency-domain,<sup>3</sup> have been used to measure chemical and biological samples, both in bulk and attached to transducer surfaces, such as planar transmission lines.<sup>4,5</sup> While interpretation of the spectra from all but the simplest samples (e.g. pure water) has been difficult, characteristic signatures of biomolecular conformation have nonetheless been observed.

Biological macromolecules exhibit weak absorptions, if any, in the microwave and terahertz regimes. Proteins are weakly dielectric, and exhibit absorption due to orientational relaxation at radio frequencies.<sup>6</sup> Double-helical DNA does not exhibit such orientational relaxation, since the dipole moments of the two helices nullify each other. Normal mode analysis predicts that both proteins<sup>7</sup> and DNA<sup>8</sup> should exhibit multiple absorptions in the terahertz range due to a variety of collective, vibrational, twisting and librational modes.

All biological macromolecules are surrounded by one or more shells of bound water<sup>6</sup>; molecules in solution are also bounded by bulk solution. Water is a strongly dielectric molecule, with absorptions throughout the microwave and terahertz regimes.<sup>9</sup> Normal mode analysis predicts multiple absorptions for water in the microwave and terahertz ranges.<sup>10</sup> Hence, the primary contributor to the absorption of any solvated biological macromolecule is water, either in bound or bulk form. The observed spectra will be a combination of absorptions from bound and/or bulk water, the biological molecule(s), and interfacial dielectric phenomena. Several authors have described responses of DNA and proteins at microwave and terahertz frequencies.<sup>11-16</sup>

Cells and tissues are complex mixtures of biological macromolecules and water. Spectra from such samples are not amenable to simple analysis,<sup>17-19</sup> but differences in hydration may be used for imaging and/or identification purposes.

### 3. Broadband stimulus/response

We focus here on coherent broadband stimulus/response measurements, working both in reflection and in transmission. While the transmission method can be used for low-loss probing through envelopes, the reflection method can be applied generally from envelopes to the human body, which cannot be imaged in transmission with terahertz systems due to high absorption of water.

To generate energy in the 1000 GHz regime, we use nonlinear transmission line (NLTL) pulse generators coupled to wideband planar antennas.<sup>20-25</sup> The GaAs IC NLTLs used in this work consist of series inductors (or sections of high-impedance transmission line) with varactor diodes periodically placed as shunt elements. On this structure at room temperature a fast ( $\sim 0.5$ -2 ps) voltage step develops from a sinusoidal input because the propagation velocity  $u$  is modulated by the diode capacitance,  $u(V) = 1/\sqrt{LC(V)}$ , where  $L$  is the line inductance and  $C(V)$  is the sum of the diode and parasitic line capacitance.<sup>24, 26</sup> Limitations of the NLTL arise from its periodic cutoff frequency, waveguide dispersion, interconnect metallization losses, and diode resistive losses. Improvements in NLTL design have resulted in sub-picosecond pulses at room temperature.<sup>25</sup>

The first electronic THz systems used resonant or broadband (bowtie) antennas driven directly by NLTLs for generation of freely propagating pulses. These pulses can be focused and collected in a manner exactly analogous to optoelectronic THz systems,<sup>27</sup> using substrate lenses and reflective optics. For coherent detection, the pulse from the receiver's NLTL was used to drive a sampler, essentially a broadband frequency mixer, whose temporal output can be sent to an oscilloscope or Fast-Fourier Transform (FFT) spectrum analyzer for display in the frequency domain.

### 4. Reflection and transmission spectroscopy with coherent detection

Increasingly sophisticated weapons and explosives require increasingly sophisticated detection technologies. Non-metallic varieties of these threats are especially important because they elude familiar metal-detecting portals, so they have motivated development of a multi-pronged approach to detection, including residue sniffing and computerized tomography. These techniques, however, have significant drawbacks, including invasiveness, slowness, unfamiliarity to the public, and significant potential for false negatives.<sup>28</sup>

Threats like these appear to be readily detectable and even identifiable using a broadband of signals in the sub-THz regime (1-500 GHz), based on experiments reported here. Traditional equipment for generating and detecting these frequencies has been difficult, bulky and expensive. The objectives of this work are to develop and apply all-electronic and monolithically integrated technology for generating and detecting these broadband signals to the problem of imaging the transmission and reflection spectra of unknown chemical or biological powders.

Many of the concepts we employ here are being pursued at lower frequencies for target detection at higher resolutions than traditional narrowband radar allows. This ultrawideband (UWB), carrier-free, impulse, or baseband radar has been rapidly gaining popularity in applications where complex and elusive targets are the norm.<sup>29</sup> UWB radar

has benefited from very recent advances in semiconductor technology enabling the production of sub-nanosecond pulses with peak powers of over 1 megawatt but having average powers in the milliwatt regime.

By contrast, the technology we employ—the integrated-circuit nonlinear transmission line (NLTL)—essentially trades power for speed, producing pico- or even sub-picosecond pulses with peak powers less than one watt and average powers in the low microwatt regime. These power levels are non-ionizing and biologically inconsequential, but because we can employ coherent detection, rejecting noise outside the frequencies of interest, we can still use them to measure useful spectra.

Baseband pico- and sub-picosecond pulses of freely propagating radiation, usually generated and coherently detected with photoconductive switches and ultrafast lasers,<sup>30-32</sup> have been useful for broadband coherent spectroscopy of materials, liquids, and gasses in the THz regime. Such systems have even been used for what could be called scale-model UWB radar.<sup>33</sup> These highly versatile beams of ultra-short electromagnetic pulses can be treated quasi-optically: They are diffracted and focused with mirrors and lenses, and the resultant effects can be readily observed in the time-domain waveform at the detector. Consequently, such beams are singularly useful for spectroscopy in a difficult-to-access spectral regime, and recent reports of spectroscopic imaging with these optoelectronic systems have generated much interest.<sup>34</sup> With these systems we have performed a variety of investigations using both transmission and reflection with a completely room-temperature system.

## 5. Sample preparation

To examine the content of envelopes with an eye toward distinguishing common powders from potentially dangerous ones, we prepared samples of sugar, starch, flour, and talcum powder. These were placed into petri dishes having 90 mm diameter and 20 mm height when covered. The masses of each sample were 56.6, 61.2, 62.0, and 84.6 grams for sugar, starch, flour, and talcum powder, respectively, and they were used in both reflection and transmission. Additional transmission measurements were done through envelopes with the same four powders and with *B. cereus*, a simulant of *B. anthracis*.

*Bacillus cereus* (from the laboratory of Dr. John Lindquist, University of Wisconsin Department of Bacteriology) was inoculated onto two tryptic soy agar plates (100 x 20 mm) as a lawn and incubated 120 hours at 27 °C. The surfaces of the plates were scraped using a flat spatula to recover spores (and residual of the vegetative cells). A slurry of this material was made by diluting it 1:1 with sterile H<sub>2</sub>O. Approximately 200 mg of spore slurry was evenly spread over a 7x10 cm piece of standard office copier paper, which was then dried at room temperature overnight.

## 6. Reflection

The reflection measurement setup is shown in Fig. 1. First, we used a copper plate with the same size of the samples to obtain a magnitude and phase reference. Each petri dish sample was collected and normalized to the reference values (Fig. 2 and Fig. 3).

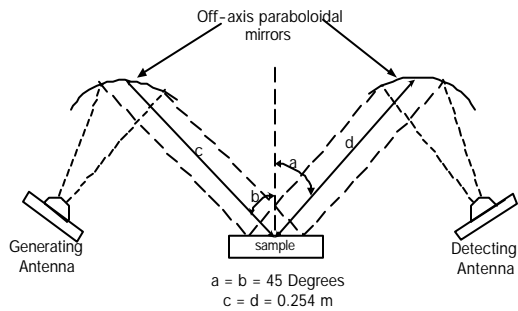


Fig. 1. Reflection measurement setup.

For both lossy and highly conducting materials, reflection measurements are preferable since transmission may not have enough signal-to-noise. As can be seen in figure 2, the reflection magnitude shows some differences in spectral patterns, part of which can be attributed to standing waves when normalized (hence the  $> 1$  reflection coefficient magnitude). The phase information, additionally, can be used to identify the sample powders.

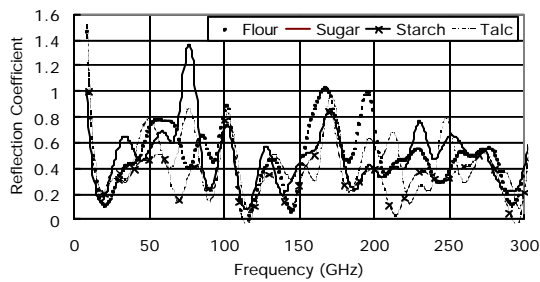


Fig. 2. Normalized reflection magnitude of common powders. Standing-wave effects at  $\sim 75$  GHz cause an anomalous peak in the ratio of the sugar sample to the empty petri dish.

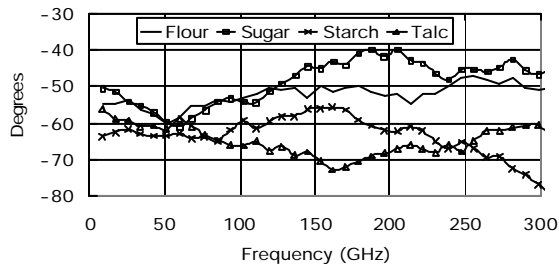


Fig. 3. Normalized, unwrapped reflection phase of common powders.

## 7. Transmission

The transmission measurement setup is shown in Fig. 4. Transmission through samples was normalized by the detected signal using empty containers in the beam path. We inserted Mylar resistive sheet attenuators into the beam path to check for uniform attenuation across the spectrum

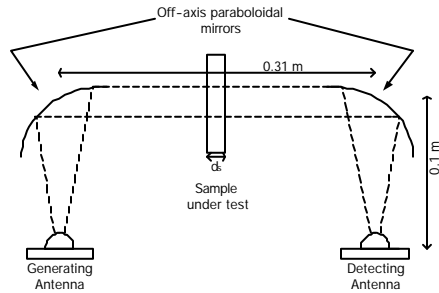


Fig. 4. Transmission measurement setup diagrams: without sample.

With this configuration we examined samples both in petri dishes and in sealed envelopes. The normalization for the petri dishes was performed by using an empty petri dish. For the envelope measurements, the reference values were taken with an empty envelope at the sample position as in Fig. 4.

We expect frequency-dependent attenuation through the samples: Fig. 5 shows more attenuation with increasing frequency than Fig. 7 because the thickness of petri dishes exceeds that of the envelopes. Furthermore, reflection measurements (Fig. 2) do not show this  $\sim 1/f$  type of attenuation. Generally, flour and starch samples have very similar patterns in the magnitude, but they are not identical. A notable result is that for both petri dish and envelope samples, the attenuation for flour and starch is larger than for the others, making identification more feasible.

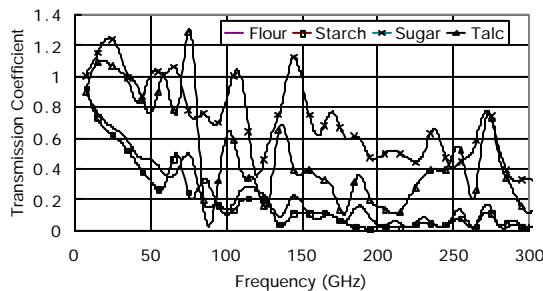


Fig. 5. Normalized transmission magnitude for samples in petri dishes. Note effects of standing waves on ratios plotted.

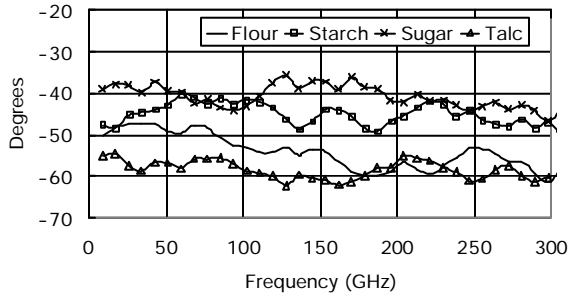


Fig. 6. Normalized and unwrapped transmission phase for samples in petri dishes.

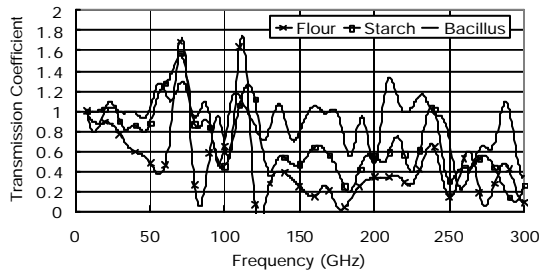


Fig. 7. Normalized transmission magnitude for samples in envelopes, comparing flour, starch, and *B. cereus* spores.

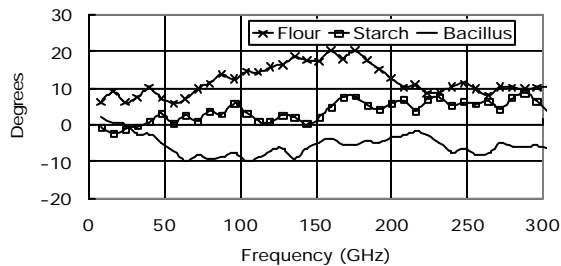


Fig. 8. Normalized and unwrapped transmission phase for samples in envelopes.

While the transmission magnitude through envelopes yields spectra that are difficult to distinguish, the phase signal has a distinctive negative dispersion characteristic of the anthrax simulant. This signal, in conjunction with measuring transmission characteristics of neighboring pixels, would provide additional information about potential threats in envelopes.

Standing-wave effects cause the ratios plotted to have magnitudes  $> 1$  at some frequencies. Inserting attenuators into the beam path could reduce this standing wave

problem, at the expense of signal-to-noise. To check for uniform attenuation, we inserted a Mylar resistive sheet (300 ohms per square) in the beam path (Fig. 9). The attenuation was 5 dB at most frequencies, but small variations are clear, and these are magnified when taking the ratio of two measurements.

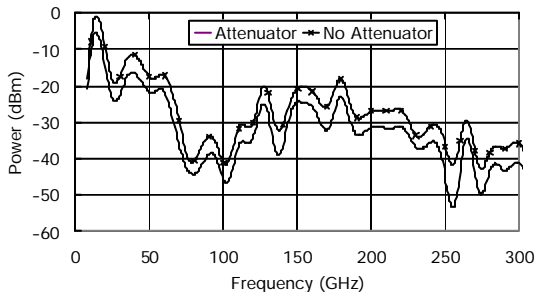


Fig. 9. Transmission with and without a 300 ohm/square attenuating sheet.

## 8. Reflection from solution proteins

In order to address uncertainties in measuring microwave interactions with biomolecules, we chose a purified protein in solution whose conformation could be thermally modulated and independently verified with optical means. Bovine pancreatic ribonuclease (RNase A), a small globular protein, was used to correlate microwave reflection measurements with changes in protein conformation. RNase A experiences reversible thermal denaturation under a variety of conditions. Conformational changes of RNase A can be detected by monitoring the UV/VIS absorbance at 288 nm.<sup>35, 36</sup> Reflection measurements from 0.5 to 6.5 GHz were performed using a resonant slot antenna attached to a vector network analyzer.<sup>37</sup> The slot antenna was attached to a fused quartz UV/VIS cuvette. A UV/VIS spectrophotometer could be used in conjunction with the antenna/cuvette assembly to obtain simultaneous optical and microwave measurements.

The presence of RNase A in solution could be detected using our slot antenna system. Fig. 10. shows a typical spectrum of RNase A; Fig. 11. shows variation of the position of a single peak with protein concentration. The peak minimum increases approximately linearly with increasing protein concentration. Note that these changes are quite small, less than 0.8 GHz over a concentration range from 0 to 2.97 mg/mL. However, this experiment demonstrates that microwave spectra are sensitive to protein concentration, as expected. This sensitivity would be expected not only for protein, but also for any solute that affects the structure of bulk water.

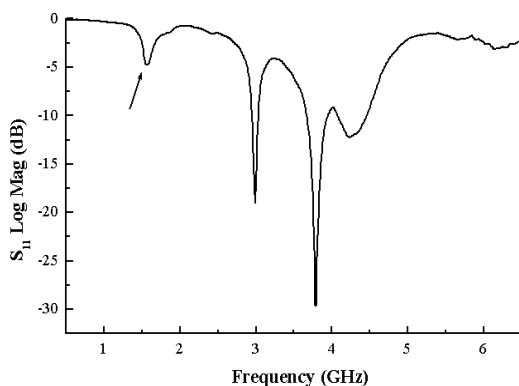


Fig. 10. Reflection spectrum from a slot antenna affixed to a cuvette with RNase-A solution. Arrow indicates a peak that is tracked in thermal measurements.

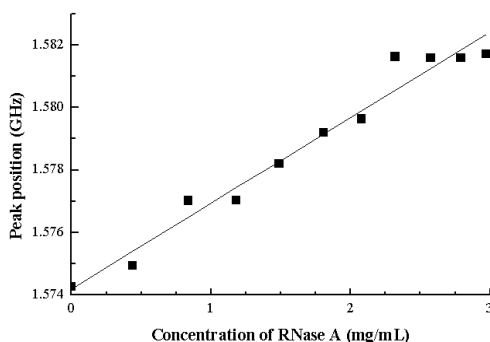


Fig. 11. Concentration dependence of frequency shift for peak noted in Fig. 10.

The response of the spectra of RNase A to increasing temperature is shown in Fig. 12. Note that peaks shift and broaden with increasing temperature. The upper half of Fig. 13 displays the response of a single peak at approximately 3.5 GHz. Note that the position of the peak minimum varies in a sinusoidal manner. Such a sinusoidal response is expected for cooperative phenomena such as protein unfolding<sup>38</sup> and is absent when buffer alone is heated under the same conditions (data not shown). This peak fitted well to a 2-state unfolding model.<sup>35</sup> Results from fitting of the peak at 3.5 GHz, and from fitting to the UV/VIS data alone, are shown in the lower half of Fig. 13. The microwave data predicts a lower midpoint temperature ( $T_m$ ) and unfolding enthalpy ( $\Delta H_m$ ) than that calculated from UV/VIS data (see Fig. 13.). Since the two data sets were obtained simultaneously, this result is probably due to differences in the phenomena being measured, not to destabilization of the protein by the microwaves. Unfolding results from UV/VIS spectroscopy in the presence and absence of microwaves are identical within experimental error, indicating that the protein is not destabilized under the conditions used (data not shown).

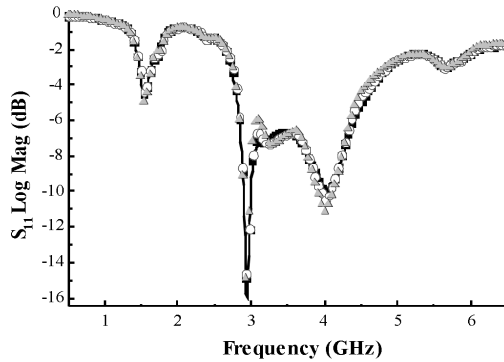


Fig. 12. Spectral response of RNase-A solution to increasing temperature.

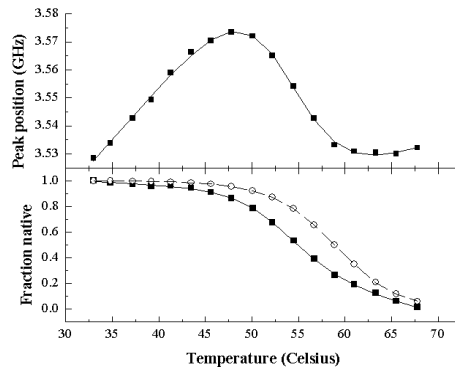


Fig. 13. Raw data from peak shift (above); data fitted to unfolding theory and compared to UV-vis absorption (open circles, below).

## 9. Future directions

To improve broadband stimulus-response measurements, both higher power systems and those with more array elements will be needed. Video-rate detection and imaging will depend on setting high enough offset frequencies between the coherent source and detector; this requires faster baseband processing.

To extend the protein solution experiments, we will perform additional unfolding at a variety of pH, concentration and microwave power conditions in order to detect limits of system and possible destabilization of the protein. Also needed are enzymology studies to ensure that activity of protein is unaffected. Other macromolecules might also be studied, such as DNA, RNA, carbohydrates and lipids. Finally, we will scale down the size of the experiment to increase the frequency to terahertz or higher.

## 10. Summary

We have discussed both broadband and resonant probing of biological samples and common powders using microwave and broadband systems. Broadband stimulus-response capabilities enable spectroscopic imaging, and increase the likelihood of sample

identification, while experiments on purified and modulated samples demonstrate conclusively the use of water bound to a protein as a label, and that the change of conformation can be observed in the perturbation of electric fields in the near zone of a slot antenna.

## 11. Acknowledgements

This work was sponsored by the United States National Science Foundation, Office of Naval Research, Air Force Office of Scientific Research and Army Research Office (Dr. D. Woolard). Kimberly Taylor is supported by an NIH Molecular Biophysics Training Grant. Earlier work on THz imaging was sponsored by the Federal Aviation Administration.

## 12. References

1. D. M. Sheen, D. L. McMakin, and T. E. Hall, "Three-dimensional millimeter-wave imaging for concealed weapon detection", *IEEE Trans. Microwave Theory Tech.* **49** (2001) 1581-92.
2. Y. Feldman, A. Andrianov, E. Polygalov, I. Ermolina, G. Romanychev, Y. Zuev, and B. Milgotin, "Time domain dielectric spectroscopy: an advanced measuring system", *Rev. Sci. Instrum.* **67** (1996) 3208-3216.
3. M. A. Hollis, C. F. Blackman, C. M. Weil, J. W. Allis, and D. J. Schaefer, "A swept-frequency magnitude method for the dielectric characterization of chemical and biological systems", *IEEE Trans. Microwave Theory Tech.* **28** (1980) 791-801.
4. J. Hefti, A. Pan, and A. Kumar, "Sensitive detection method of dielectric dispersions in aqueous-based, surface-bound macromolecular structures using microwave spectroscopy", *Appl. Phys. Lett.* **75** (1999) 1802-1804.
5. G. R. Facer, D. A. Notterman, and L. L. Sohn, "Dielectric spectroscopy for bioanalysis: From 40 Hz to 26.5 GHz in a microfabricated wave guide", *Appl. Phys. Lett.* **78** (2001) 996-998.
6. R. Pethig, *Dielectric and electronic properties of biological materials*. John Wiley & Sons, Chichester, 1979.
7. F. Tama, F. X. Gadea, O. Marques, and Y. H. Sanejouand, "Building-block approach for determining low-frequency normal modes of macromolecules", *Proteins-Structure Function and Genetics*. **41** (2000) 1-7.
8. M. Bykhovskaia, B. Gelmont, T. Globus, D. L. Woolard, A. C. Samuels, T. H. Duong, and K. Zakrzewska, "Prediction of DNA far-IR absorption spectra based on normal mode analysis", *Theoretical Chemistry Accounts*. **106** (2001) 22-27.
9. D. J. Segelstein, "The complex refractive index of water." University of Missouri, Kansas City 1981.
10. J. T. Kindt and C. A. Schmuttenmaer, "Far-infrared absorption spectra of water, ammonia, and chloroform calculated from instantaneous normal mode theory", *J. Chem. Phys.* **106** (1997) 4389-4400.
11. R. Pethig, "Protein-Water Interactions Determined by Dielectric Methods", *Annual Review of Physical Chem.* **43** (1992) 177-205.
12. A. G. Markelz, A. Roitberg, and E. J. Heilweil, "Pulsed terahertz spectroscopy of DNA, bovine serum albumin and collagen between 0.1 and 2.0 THz", *Chemical Phys. Lett.* **320** (2000) 42-48.
13. N. Nandi, K. Bhattacharyya, and B. Bagchi, "Dielectric relaxation and solvation dynamics of water in complex chemical and biological systems", *Chemical Reviews*. **100** (2000) 2013-2045.
14. K. Taylor and D. W. van der Weide, "Microwave assay for detecting protein conformation in solution", presented at Photonics Boston, Boston, 2001.

15. K. Taylor and D. W. van der Weide, "Sensing folding of solution proteins with resonant antennas", presented at 9th International Conference on Terahertz Electronics, Charlottesville, 2001.
16. C. Wichaidit, J. R. Peck, Z. Lin, R. J. Hamers, S. C. Hagness, and D. W. van der Weide, "Resonant slot antennas as transducers of DNA hybridization: A computational feasibility study", *IEEE MTT-S Int. Microwave Symp. Dig.* **1** (2001) 163-166.
17. P. Y. Han and X. C. Zhang, "Time-domain spectroscopy targets the far-infrared", *Laser Focus World.* **36** (2000) 117-+.
18. S. W. Smye, J. M. Chamberlain, A. J. Fitzgerald, and E. Berry, "The interaction between Terahertz radiation and biological tissue", *Phys. Med. Biol.* **46** (2001) R101-R112.
19. A. J. Fitzgerald, E. Berry, N. N. Zinovev, G. C. Walker, M. A. Smith, and J. M. Chamberlain, "An introduction to medical imaging with coherent terahertz frequency radiation", *Phys. Med. Biol.* **47** (2002) R67-R84.
20. D. W. van der Weide, J. S. Bostak, B. A. Auld, and D. M. Bloom, "All-electronic free-space pulse generation and detection", *Electronics Lett.* **27** (1991) 1412-1413.
21. D. W. van der Weide, J. S. Bostak, B. A. Auld, and D. M. Bloom, "All-electronic generation of 880 fs, 3.5 V shockwaves and their application to a 3 THz free-space signal generation system", *Appl. Phys. Lett.* **62** (1993) 22-24.
22. Y. Konishi, M. Kamegawa, M. Case, R. Yu, M. J. W. Rodwell, and R. A. York, "Picosecond electrical spectroscopy using monolithic GaAs circuits", *Appl. Phys. Lett.* **61** (1992) 2829-2831.
23. Y. Konishi, M. Kamegawa, M. Case, Y. Ruai, S. T. Allen, and M. J. W. Rodwell, "A broadband free-space millimeter-wave vector transmission measurement system", *IEEE Trans. Microwave Theory Tech.* **42** (1994) 1131-1139.
24. M. J. W. Rodwell, S. T. Allen, R. Y. Yu, M. G. Case, U. Bhattacharya, M. Reddy, E. Carman, M. Kamegawa, Y. Konishi, J. Puhl, R. Pallela, and J. Esch, "Active and nonlinear wave propagation devices in ultrafast electronics and optoelectronics (and prolog)", *Proc. IEEE.* **82** (1994) 1035-59.
25. D. W. van der Weide, "Delta-doped Schottky diode nonlinear transmission lines for 480-fs, 3.5-V transients", *Appl. Phys. Lett.* **65** (1994) 881-883.
26. M. J. W. Rodwell, M. Kamegawa, R. Yu, M. Case, E. Carman, and K. S. Giboney, "GaAs nonlinear transmission lines for picosecond pulse generation and millimeter-wave sampling", *IEEE Trans. Microwave Theory Tech.* **39** (1991) 1194-204.
27. M. C. Nuss and J. Orenstein, "Terahertz time-domain spectroscopy", in *Millimeter and Submillimeter Wave Spectroscopy of Solids*, vol. 74, *TOPICS IN CURRENT CHEMISTRY*, 1998, pp. 7-50.
28. P. Mann, "TWA disaster reopens tough security issues", in *Aviation Week & Space Technology*, vol. 145, 1996, pp. 23-27.
29. D. Herskovitz, "Wide, Wider, Widest", *Microwave Journal.* **38** (1995) 26-40.
30. M. v. Exeter, "Terahertz time-domain spectroscopy of water vapor", *Optics Lett.* **14** (1989) 1128-1130.
31. D. Grischkowsky, S. Keiding, M. v. Exeter, and C. Fattinger, "Far-infrared time-domain spectroscopy with terahertz beams of dielectrics and semiconductors", *Journal of the Optical Society of America B.* **7** (1990) 2006-2015.
32. M. C. Nuss, K. W. Goossen, J. P. Gordon, P. M. Mankiewich, M. L. O'Malley, and M. Bhusan, "Terahertz time-domain measurement of the conductivity and superconducting band gap in niobium", *J. Appl. Phys.* **70** (1991) 2238-2241.
33. R. A. Cheville and D. Grischkowsky, "Time domain terahertz impulse ranging studies", *Appl. Phys. Lett.* **67** (1995) 1960-1962.
34. B. B. Hu and M. C. Nuss, "Imaging with terahertz waves", *Optics Lett.* **20** (1995) 1716-1718.
35. T. A. Klink, K. J. Woycechowsky, K. M. Taylor, and R. T. Raines, "Contribution of disulfide bonds to the conformational stability and catalytic activity of ribonuclease A", *European Journal of Biochemistry.* **267** (2000) 566-572.

36. C. N. Pace, G. R. Grimsley, S. T. Thomas, and G. I. Makhatadze, "Heat capacity change for ribonuclease A folding", *Protein Science*. **8** (1999) 1500-1504.
37. H. G. Akhavan and D. Mirshekar-Syahkal, "Slot antennas for measurement of properties of dielectrics at microwave frequencies", presented at National Conference on Antennas and Propagation, 1999.
38. T. E. Creighton, *Proteins: structures and molecular properties*, Second ed. New York: W.H. Freeman and Company, 1993.